CHAPTER-3

SEGMENTATION OF BLOOD VESSELS FROM DIGITAL FUNDUS IMAGES

Ocular fundus image assessment has been extensively used by ophthalmologists for diagnosing vascular and non vascular pathology. Examining the retinal blood vessel network may reveal arteriosclerosis, diabetes, hypertension, cardiovascular disease and stroke [12]. Furthermore, the segmentation of the vessel network is the most suitable representation for the retinal image registration since vascular tree does not change except in a few diseases and includes adequate information for the identification of some anchor points. In addition, vessel tree can also be used as a land mark feature for image-guided laser treatment of choroidal neovascularization. Therefore reliable methods for segmentation of blood vessels in fundus images are needed.

The methods used for blood vessel segmentation discussed in Chapter-2 can work well to segment the major parts of the blood vessels. However, the major challenges confronting the vessel segmentation methods which are shown in Fig. 3.1are:

- Segmentation of the thinner blood vessels as the image contrast is normally low around thin blood vessels;
- The presence of pathologies as they may be mis-enhanced and mis-detected as vessels.

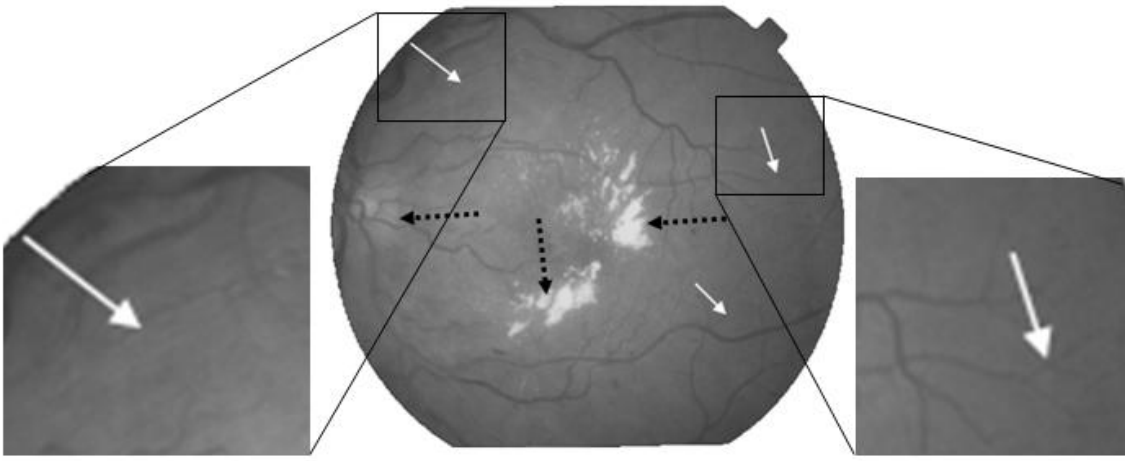

Fig.3.1. Challenges in Extraction of Retinal Vasculature having Severe Pathology from STARE Database. Arrows drawn on the image in black dashed lines show lesions and the boundary of the optic disc., Arrows drawn in white lines highlight narrow blood vessels in low contrast regions.

In order to solve these problems, Histogram Matched Local Relative Entropy (HMLRE) method is developed to segment blood vessels in fundus images. For efficient detection of vasculature, high contrast between vessel network and the fundus background is desired while there must be low contrast between the fundus background and retinal pathologies [93]. In red channel of a RGB colour image, the gray levels are spread over a wider range compared to green channel. Therefore the contrast between bright pathologies and fundus background is less in red channel. Thus in HMLRE method, red channel's intensity information is used in pre-processing of colour fundus images. The histogram of green channel is modified by employing the histogram of red channel (of the same fundus image) to

obtain a new image in preprocessing. The contrast of vasculature against the background of the preprocessed image is improved by using matched filter. The local relative entropy thresholding with histogram compression and translation is employed to discriminate blood vessel segments from the background in the matched filter response. The misclassified pixels are then removed by using label filtering. The performance of the proposed HMLRE method is evaluated on the publicly available STARE [20] and DRIVE [94] databases using Receiver Operating Characteristic (ROC) curve analysis. Experimental evaluation of the HMLRE method demonstrates substantial performance over other blood vessel segmentation algorithms recently reported in the literature.

This chapter is structured as follows. In Section 3.1, the HMLRE method is presented. Implementation details of HMLRE method are described in Section 3.2. Experimental results are presented and compared with existing methods in Section 3.3. Conclusions are given in Section 3.4.

3.1. PROPOSED ALGORITHM

The proposed HMLRE method consists of four steps as shown in fig. 3.2. Firstly, the histogram of green channel is modified by employing the histogram of red channel (of the same fundus image) to obtain a new preprocessed image. Secondly, to enhance the blood vessels in the histogram matched image a 2D matched filter kernel is applied. Then, local relative entropy thresholding is used to

differentiate blood vessel segments from the background in the matched filter response image. Finally, label filtering is exploited to remove the misclassified pixels.

Histogram matching is applied to make use of the intensity information of red and green channels. The intensity information of red channel is used for two reasons:

- To enhance the visual appearance of fundus images in cases of varying illumination.
- To improve the performance of blood vessel segmentation.

Therefore the histogram of the green channel is modified by using the histogram of red channel (of the same fundus image) to attain a new image.

To improve the contrast of vasculature against the fundus background, matched filter is employed. In order to properly segment the enhanced vessel segments in the matched filter response images, an effective thresholding scheme is necessary. An efficient local relative entropy based thresholding method that takes into account the spatial distribution of gray levels is used, because some matched filter response images have complicated relationships or overlap between foreground and background. Particularly, thresholding based on local relative entropy [95] is implemented which can well maintain the structure details of an image. Connected component labeling is applied to identify individual objects in each relative local entropy thresholded image. Connected component labeling is an image

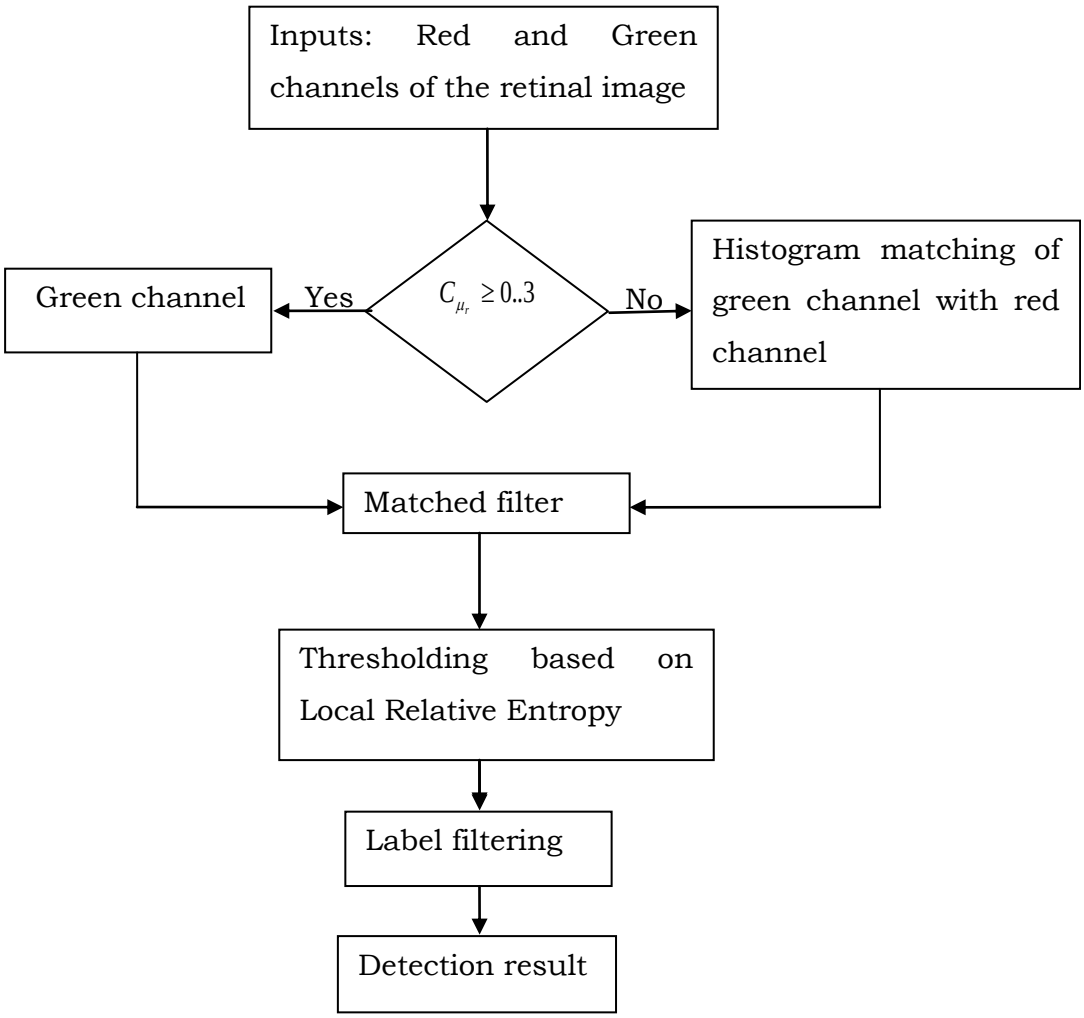

Fig.3.2. Flow Chart of the Proposed HMLRE Method

analysis method that scans an image pixel by pixel. It groups all the pixels into components depending on pixel connectivity. The label filtering attempts to separate the individual objects by make use of the eight connected neighborhood information and label propagation.

3.2. IMPLEMENTATION DETAILS

The implementation details of the proposed HMLRE method are explained in this section.

3.2.1. PREPROCESSING USING HISTOGRAM MATCHING

For extracting blood vessel network, the unsupervised methods generally use the green channel of the colour fundus image as it has the best vessel/background contrast. The red channel of the colour fundus image has the following advantages;

- The red channel is brighter.
- In red channel the gray level values are spread over a wider range.

This results in less contrast between pathologies and retinal background that can be observed in Fig. 3.3. Hence in the proposed HMLRE method, intensities of both the red and green channels of the same fundus image are utilized. Histogram matching is applied to modify the histogram of green channel by employing the histogram of red channel (of the same fundus image) to get a new image that have the advantages of both the channels. For retinal images having very high brightness, histogram matching of green and red channel images

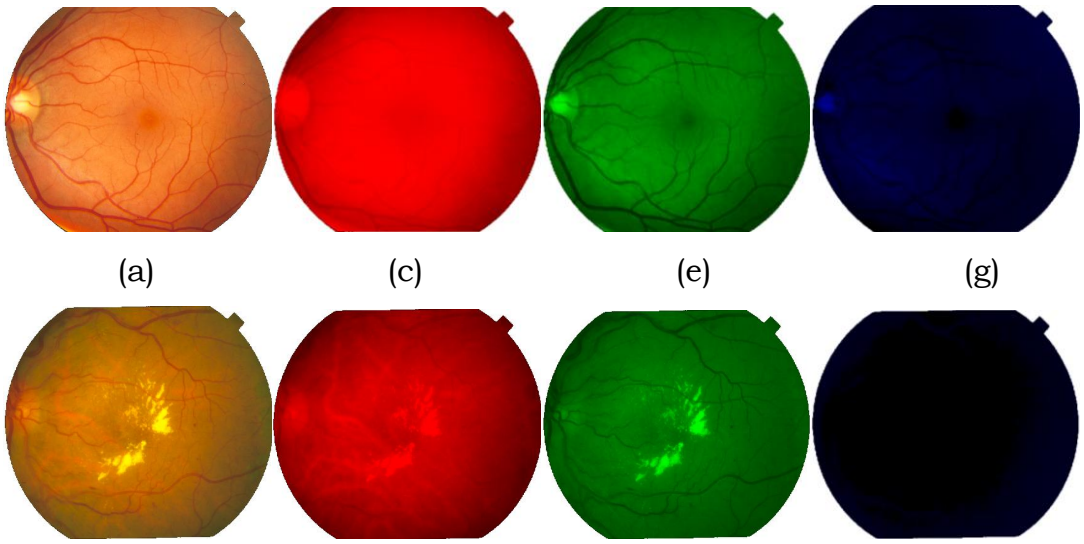

Fig.3.3. (a) Healthy Colour Retinal Image (b) Colour Retinal Image with Severe Pathology (c) & (d) Red Channel Images (e) & (f) Green Channel Images (g) & (h) Blue Channel Images.

reduces the contrast between vasculature and its background. This leads to an image with low contrast than the contrast in the green channel. In these cases, green channel images are preferred over the histogram matched images. To overcome this problem a condition is applied whether to use histogram matching or not. The condition to use green channel of a colour fundus image is $C_{\mu_r} \geq 0.3$,

where $\mu_r = \sum_{j=0}^{L-1} r_j . P_r(r_j)$ $C_k = \sum_{j=0}^{k} P_r(r_j)$ (3.1)

$P_r(r)$ corresponds to the probability density function of the red channel of the colour image,

L indicates the number of discrete gray levels, and

k refers to the bin having the mean value μ_r.

The value of *C* characterizes the set of very bright images with a large gap in their histograms. Figures 3.4 and 3.5 explain the affect of histogram matching. There is a substantial decrease in contrast between abnormalities and the retinal background which can be observed from Figs. 3.4 and 3.5.

3.2.2. MATCHED FILTER

The retinal vasculature has the following three important properties that are useful for blood vessel analysis [18]:

1. The blood vessels may be approximated as piecewise linear segments as they have small curvatures.
2. The reflectance of blood vessels is low compared to other retinal surfaces. So the blood vessels appear darker relative to the background. Even though the intensity profile of a vessel differs from another vessel by a small amount, the intensity profile of a blood vessel can be approximated using a Gaussian shaped curve,

$$f(x,y) = A\{1 - k\exp(-\frac{d^2}{2\sigma^2})\}, \qquad (3.2)$$

where *d* refers to the perpendicular distance between a point *(x, y)* and the straight line that passes through the center of blood vessel in a direction towards its length, σ is the spread of the intensity profile, *A* defines local background's gray level

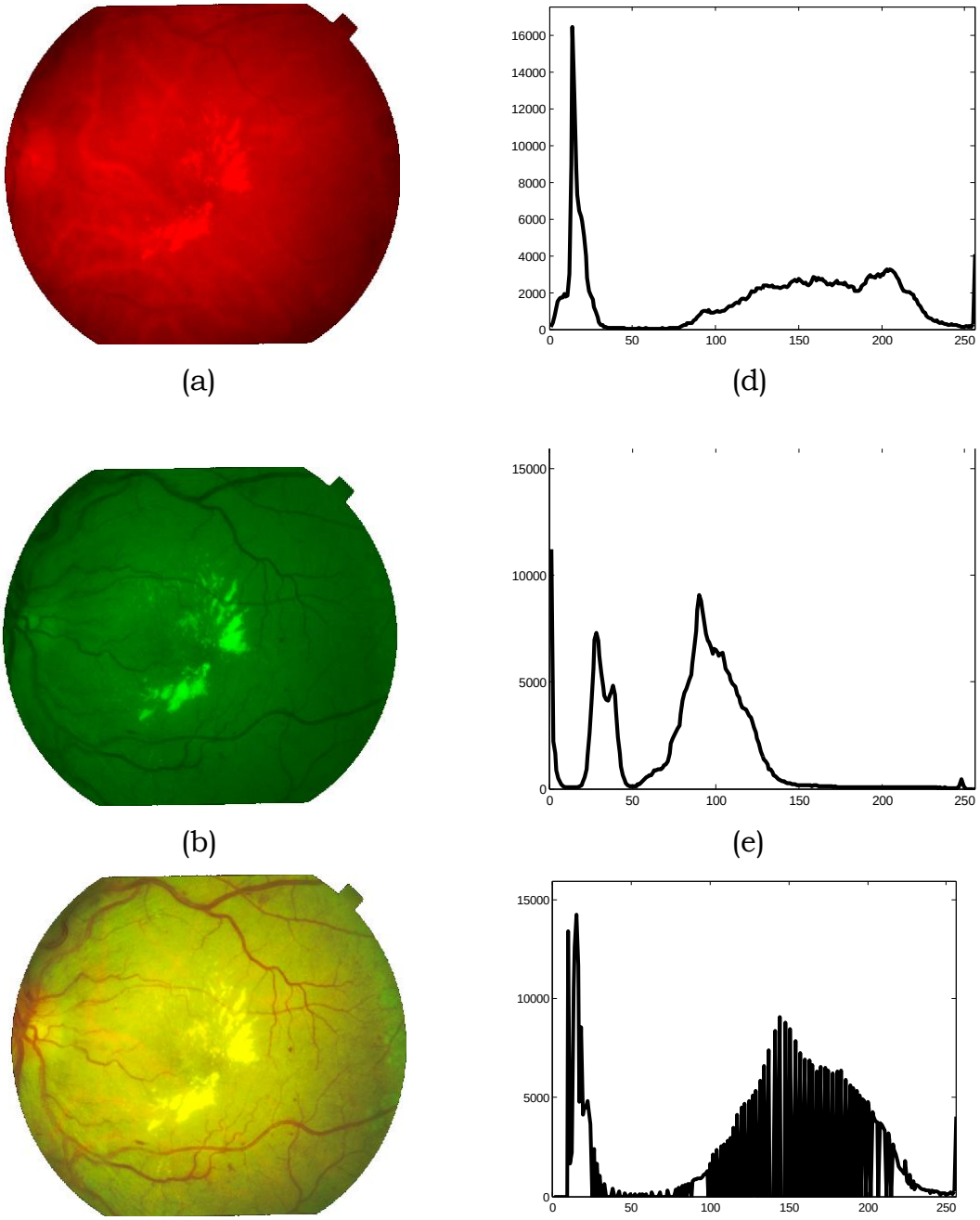

Fig.3.4. Fundus Image Preprocessing to Decrease the Contrast between Abnormalities and the Retinal Background (a) Red Channel of a Fundus Image; (b) Green Channel of the Same Image; (c) Histogram Matched Image; Gray-Level Distributions of the Same Fundus Image (d) Red Channel; (e) Green Channel; and (f) Histogram Matched Image.

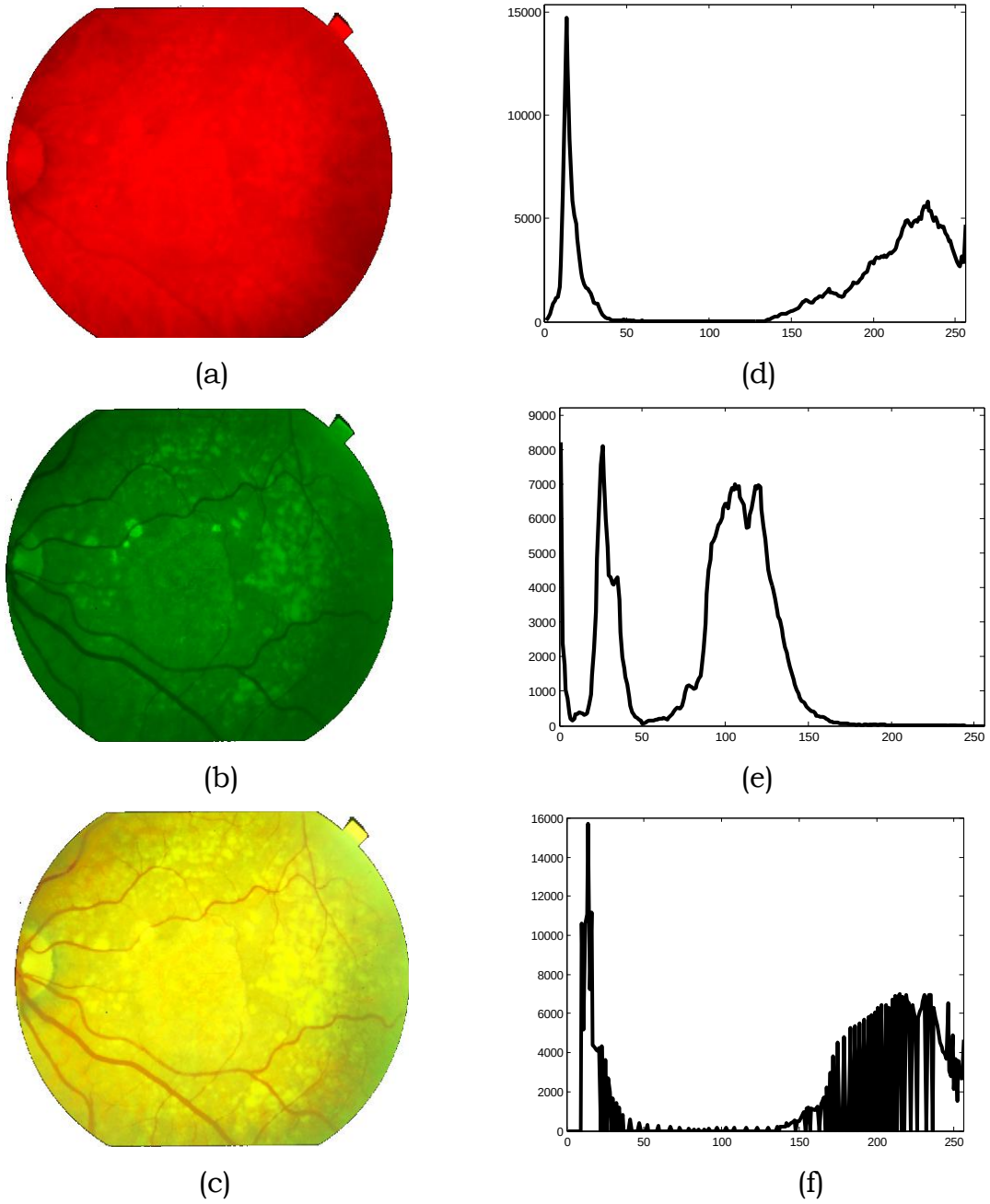

Fig.3.5. Fundus Image Preprocessing to Decrease the Contrast between Abnormalities and the Retinal Background (a) Red Channel of a Fundus Image; (b) Green Channel of the Same Image; (c) Histogram Matched Image; Gray-Level Distributions of the Same Fundus Image (d) Red Channel; (e) Green Channel; and (f) Histogram Matched Image.

intensity and k indicates the measure of reflectance of the vessel relative to its neighborhood.

3. The width of a blood vessel decreases as it goes radially outward from the optic disk.

Therefore, a blood vessel is defined as a dark pattern having Gaussian shape cross-section profile, piecewise connected, and locally linear.

Because of the above mentioned properties, instead of matching a single intensity profile of the blood vessel cross-section, a considerable improvement can be attained by matching number of cross-sections of similar profile simultaneously. A prototype of the matched filter kernel is expressed as

$$k(x,y) = -\exp(-\frac{x^2}{2\sigma^2}) \qquad \text{for} \quad |y| \le L/2. \tag{3.3}$$

Where l indicates the length of blood vessel segment for which the blood vessel is having a fixed orientation. The direction of the blood vessel is considered to be aligned along the y-axis. The matched filter kernel is required to be rotated for all possible angles since a blood vessel may be oriented at any angle. Twelve 15 x 15 pixel kernels are applied to convolve with a fundus image. At each pixel only the maximum of their responses is retained. The results after convolving matched filter kernels at different angles with green channel of the histogram matched image in fig. 3.5 (c) are shown in fig.3.6. The

matched filter response image for the image in fig. 3.5 (c) is shown in fig. 3.7(a), where the blood vessels are significantly enhanced.

3.2.3. LOCAL RELATIVE ENTROPY THRESHOLDING WITH HISTOGRAM COMPRESSION AND TRANSLATION

In order to properly segment the enhanced blood vessel segments in the matched filter response images, an effective thresholding scheme is required. An efficient relative entropy based thresholding algorithm that takes into account the spatial distribution of gray levels is used, because some matched filter response images have complicated relationships or overlap between foreground and background. Particularly, local relative entropy thresholding method [95] is implemented that can well maintain the structure details in the thresholded image.

The co-occurrence matrix of an image is defined as a $L \times L$ square matrix, represented by $W = \left[t_{ij} \right]_{L \times L}$ whose elements are specified by the number of gray level transitions between all pairs is $G = \{0,1,...,L-1\}$ in a particular way. Different definitions are possible for a co-occurrence matrix depending on the way the gray level *i* follows the gray level *j*. One extensively employed co-occurrence matrix is an asymmetric matrix that considers only the transitions of gray level between two adjacent pixels. Thus, t_{ij} is defined as follows:

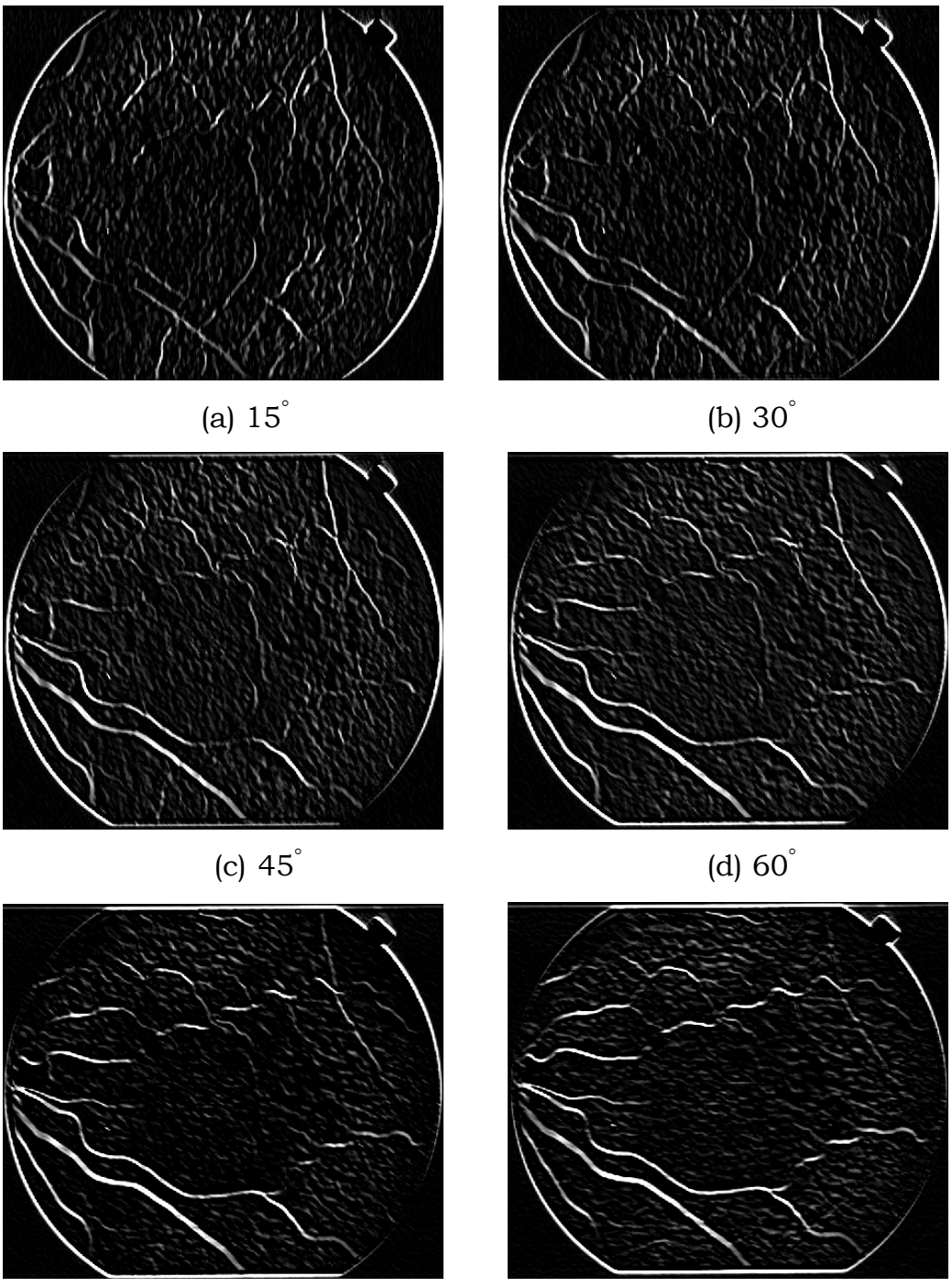

(a) 15° (b) 30°

(c) 45° (d) 60°

(e) 75° (f) 90°

Fig.3.6. Results after Convolving Matched Filter Kernels at Different Angles with Green Channel of the Histogram Matched Image Shown in Fig. 3.5 (c).

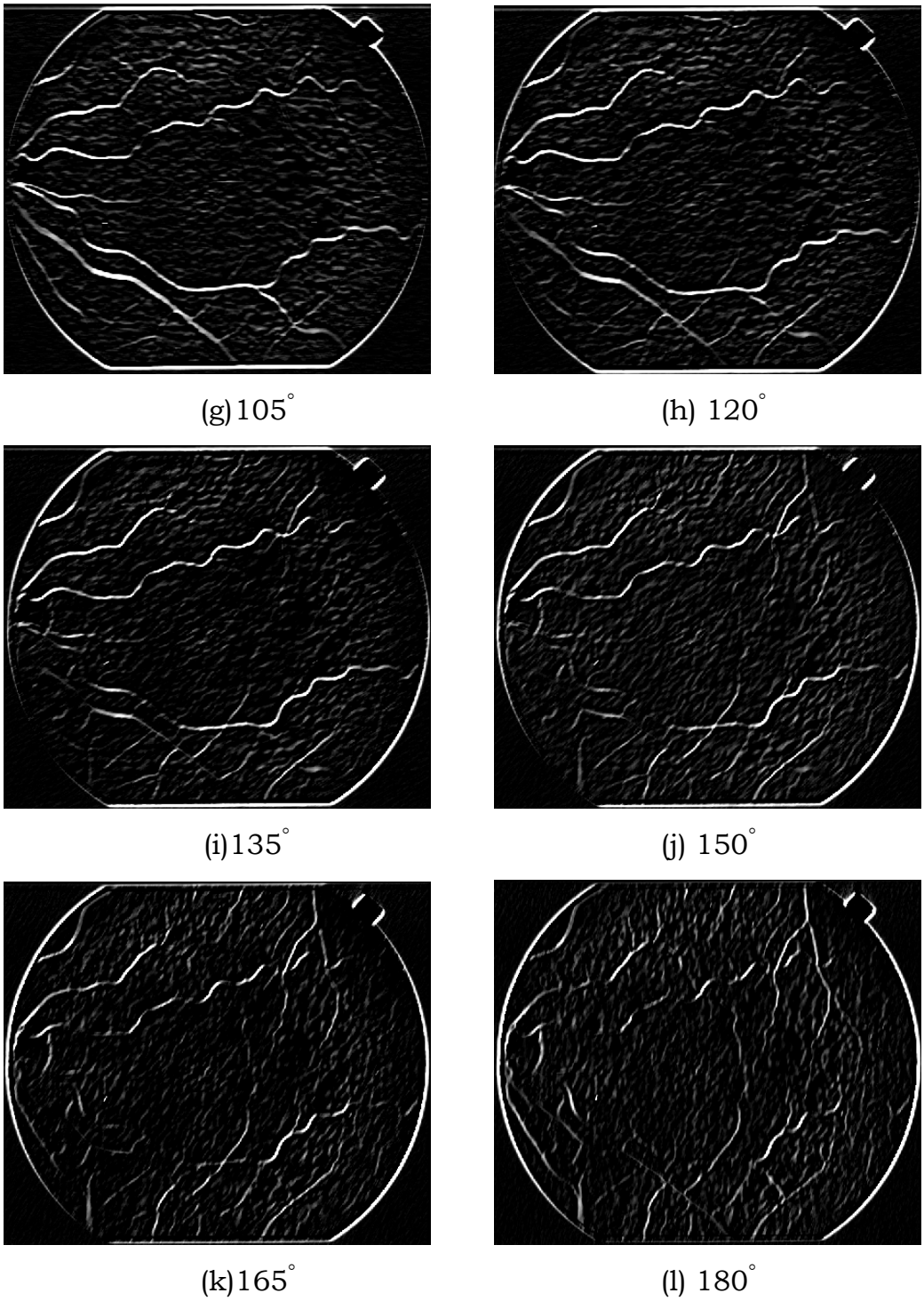

(g) 105° (h) 120°

(i) 135° (j) 150°

(k) 165° (l) 180°

Fig.3.6. Results after Convolving Matched Filter Kernels at Different Angles with Green Channel of the Histogram Matched Image Shown in Fig. 3.5 (c).

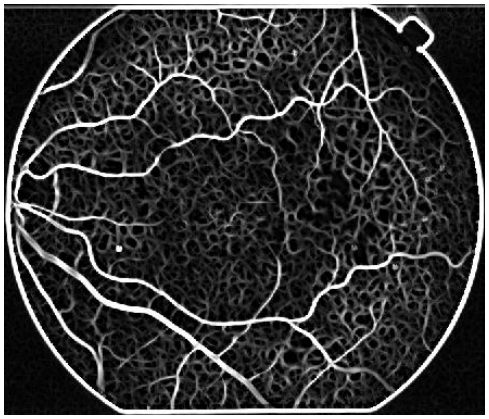

(A)

(B)

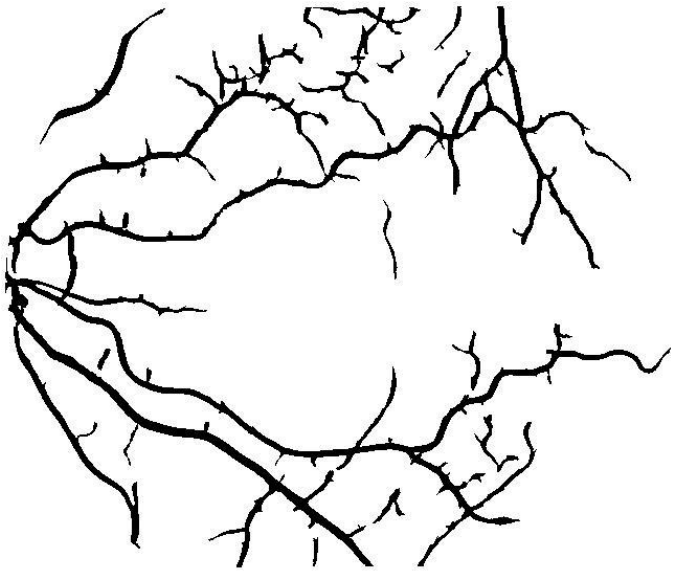

(c)

Fig.3.7. (a) Matched Filter Response of the Histogram Matched Image (b) Result after Local Relative Entropy Thresholding with HCT (c) Label Filtering Result.

A (BB)	B (BF)
D (FB)	C (FF)

Fig.3.8. Quadrants of Co-occurrence Matrix [95]

$$t_{ij} = \sum_{m=1}^{M} \sum_{n=1}^{N} \delta_{mn} \tag{3.4}$$

where $\delta_{mn} = 1$ if $\begin{cases} f(m,n) = i \text{ and } f(m+1,n) = j \\ \text{and/or} \\ f(m,n) = i \text{ and } f(m,n+1) = j \end{cases}$

$= 0$ otherwise

The desired gray level *i* from gray level *j* can be attained by normalizing the total number of transitions in co-occurrence matrix.

$$p_{ij} = \frac{t_{ij}}{\sum_{k=0}^{L-1} \sum_{l=0}^{L-1} t_{kl}} \tag{3.5}$$

Let an image be thresholded by a value *t*. The co-occurrence matrix will be partitioned into four quadrants using this threshold, namely, A, B, C and D as shown in Fig.3.8. Here, it is assumed that pixels having gray level above the threshold value are assigned to foreground (corresponding to objects). Pixels having gray level equal to or below the threshold value are allocated to the background.

The cell probabilities in each quadrant can be obtained by normalization,

$$p^t_{ij|A} = \frac{p_{ij}}{P^t_A},\ p^t_{ij|B} = \frac{p_{ij}}{P^t_B},\ \ p^t_{ij|C} = \frac{p_{ij}}{P^t_C},\ \ p^t_{ij|D} = \frac{p_{ij}}{P^t_D} \tag{3.6}$$

where P^t_A, P^t_B, P^t_C and P^t_D are the probabilities associated with each quadrant. Let "t" is the selected threshold value. Let h^t_{ij} is the transition probability of the t-thresholded image in response to p_{ij}. The corresponding cell probabilities in each of four quadrants of a thresholded image are given by [95]

$$h^t_{ij|A} = q^t_A = \frac{P^t_A}{(t+1)(t+1)} \qquad h^t_{ij|B} = q^t_B = \frac{P^t_B}{(t+1)(L-1-t)} \tag{3.6.a}$$

$$h^t_{ij|C} = q^t_C = \frac{P^t_C}{(L-t-1)(L-t-1)} \qquad h^t_{ij|D} = q^t_D = \frac{P^t_D}{(L-t-1)(t+1)}$$

The relative entropy between the probability distributions $\{p_{ij}\}_{i=0,j=0}^{L-1,L-1}$ and $\{h^t_{ij}\}$ is defined as

$$J(\{p_{ij}\},\{h^t_{ij}\}) = \sum_{i=0}^{L-1}\sum_{j=0}^{L-1} p_{ij}\log\frac{p_{ij}}{h^t_{ij}}$$

$$= -H(\{p_{ij}\}) - (P^t_A \log q^t_A + P^t_B \log q^t_B + P^t_C \log q^t_C + P^t_D \log q^t_D) \tag{3.7}$$

where $H(\{p_{ij}\})$ is the entropy of the probability vector specified by $\{p_{ij}\}_{i=0,j=0}^{L-1,L-1}$ and is independent of t.

If $p_{ij|AC}^{t} = p_{ij} / \left(P_A^t + P_C^t\right)$ then the local relative entropy thresholding is given by

$$J_{LRE}\left(\{p_{ij|AC}\}; h_{ij}^{t}\right) = -H_{BB+FF}(t) - \sum_{(i,j)\in BB\cup FF} p_{ij|AC} \log h_{ij}^{t} \qquad (3.8)$$

Where $-H_{BB+FF}(t) = -\sum_{(i,j)\in BB\cup FF} p_{ij|AC}$ refers to the entropy of the local quadrants *A* and *C*.

Reducing the second term in equation (3.8) further results in

$$J_{LRE}\left(\{P_{ij|AC}\}; h_{ij}^{t}\right) = -H_{BB+FF}(t) - \left[\frac{P_A^t}{P_A^t + P_C^t}\log\left(\frac{q_A^t}{P_A^t + P_C^t}\right) + \frac{P_C^t}{P_A^t + P_C^t}\log\left(\frac{q_C^t}{P_A^t + P_C^t}\right)\right] \qquad (3.9)$$

The LRE thresholding technique is to find a threshold value t_{LRE} that minimizes $J_{LRE}\left(\{P_{ij\setminus AC}\}; h_{ij}^{t}\right)$ [95], that is

$$t_{LRE} = \arg\left\{\min_{t\in G} J_{LRE}\left(\{P_{ij\setminus AC}\}; h_{j}^{t}\right)\right\} \qquad (3.10)$$

Generally relative entropy based methods are liable to sparse image histograms. To make the relative entropy based methods work efficiently, a sparse image histogram have to be compressed to a more compact histogram. This is known as Histogram Compression and

Translation (HCT). Assume that an image contains 'n' number of distinct gray levels. Without loss of generality, supposing $g_1, g_2, \ldots, g_N$ are the N different gray levels which can be set in accordance with $g_1 < g_2 < \ldots g_N$, where $g_1 = g_{min}$ is the smallest gray level and $g_N = g_{max}$ is the largest gray level. Assume that $n(g_k)$ indicates total number of pixels in the fundus image that are having gray level g_k. The process of histogram compression and translation is described by mapping $g_k \rightarrow k$ with HCT $(g_k) = k$ and $n_k = n(g_k)$ for each $1 \leq k \leq N$. For the matched filter response image shown in Fig. 3.7(a), the local relative entropy based thresholding with histogram compression and translation result is shown in Fig. 3.7(b) where the blood vessels are clearly segmented from the background.

3.2.4. LABEL FILTERING

As seen in Fig. 3.7(b), there are still some misclassified pixels in the image. The aim of label filtering is to produce a clean and complete blood vessel network by removing misclassified pixels by using the concept of connected component labeling. Connected regions correspond to individual objects. Hence, connected regions must be identified first. Connected component labelling scans an image pixel by pixel. It groups all the scanned pixels into components based on pixel connectivity. The label filtering tries to separate the individual objects by using eight connected neighborhood information and label propagation [96]. Once the algorithm is executed, only the resulting components exceeding a certain number of pixels, e.g., 200 are

labeled as blood vessels. Fig. 3.7(c) shows the results after label filtering.

3.3. EXPERIMENTAL RESULTS AND DISCUSSION

The proposed HMLRE method is tested on two publicly available databases of coloured fundus images and corresponding groundtruth segmentations: the DRIVE [94] and STARE [20] databases. The DRIVE database contains 40 colour fundus images. The images are divided into 20 test and 20 training images of size 565 x 584 pixels. The fundus images have been manually segmented by three experts. The fundus images in the training set are segmented once, while the images in the test set are segmented two times, resulting in sets A and B. The STARE database consists of 20 fundus images which are of size 700 x 605 pixels, 8 bits per colour channel. Among the 20 images of STARE database, 10 images are of patients with no lesions (normals) and the other 10 images contain lesions that obscure or confuse the blood vessel appearance in varying positions of the fundus image (abnormals). All the images are segmented for blood vessels by two ophthalmic experts.

In order to evaluate the proposed HMLRE method three performance measures are employed. The first is ROC that is used to plot the variation of false positive rate (F_p) against true positive rate (T_p).

$$T_P = \frac{N_{tp}}{N_{vessel}} \; ; \quad F_P = \frac{N_{fp}}{N_{non-vessel}} \tag{3.11}$$

where N_{tp}, N_{fp} define the number of true positives and false positives. N_{vessel}, $N_{non-vessel}$ are the total number of blood vessel and non-blood vessel pixels in the groundtruth image. The second performance measure is the area under the ROC. High area under ROC indicates the better detection. The detection is perfect, if the area under ROC is one. The third measure is the average accuracy for all fundus images. The accuracy of an image can be found using the following expression.

$$Accuracy = \frac{\text{Sum of the total number of pixels, correctly classified as vessel and non-vessel pixels}}{\text{Total number of pixels in the field of view of the fundus image}}$$

A fundus image having severe pathology shown in Fig. 3.9(a) is utilized to compare the performance of the HMLRE method with other methods. In all the other blood vessel segmentation approaches whether it is supervised or unsupervised, the abnormalities are mis-enhanced and mis-detected as blood vessels. From Fig.3.9, it can be examined that, the proposed HMLRE method avoided detecting false vessels in abnormal regions and produced reliable results for healthy regions successfully**.**

Illustrative segmentation results of the HMLRE method for a pair of fundus images from DRIVE database together with manual segmentations are shown in Figs. 3.10 and 3.11. The accuracy for the

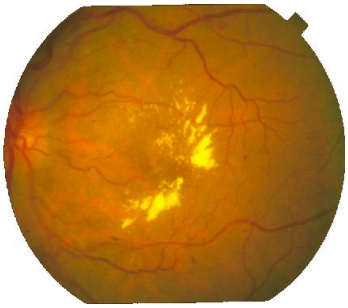

(a) Retinal image with pathology

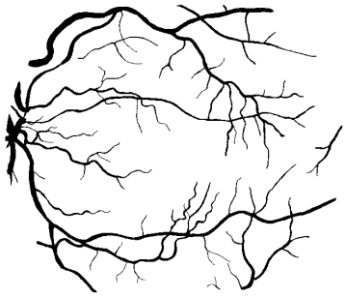

(b) First observer

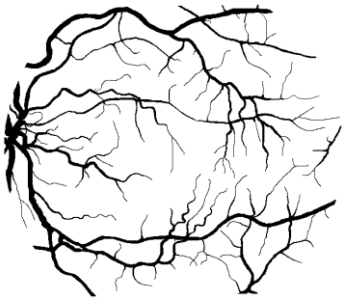

(c) Second observer

(d) Result of Soares *et al.*[48]

(e)Result of Hoover *et al.*[20]

(f) Result of Jiang *et al.*[51]

(g) Result of proposed method.

Fig.3.9. Comparison of Results on a Retinal Image having Severe Pathology shown in Fig. 3.1.

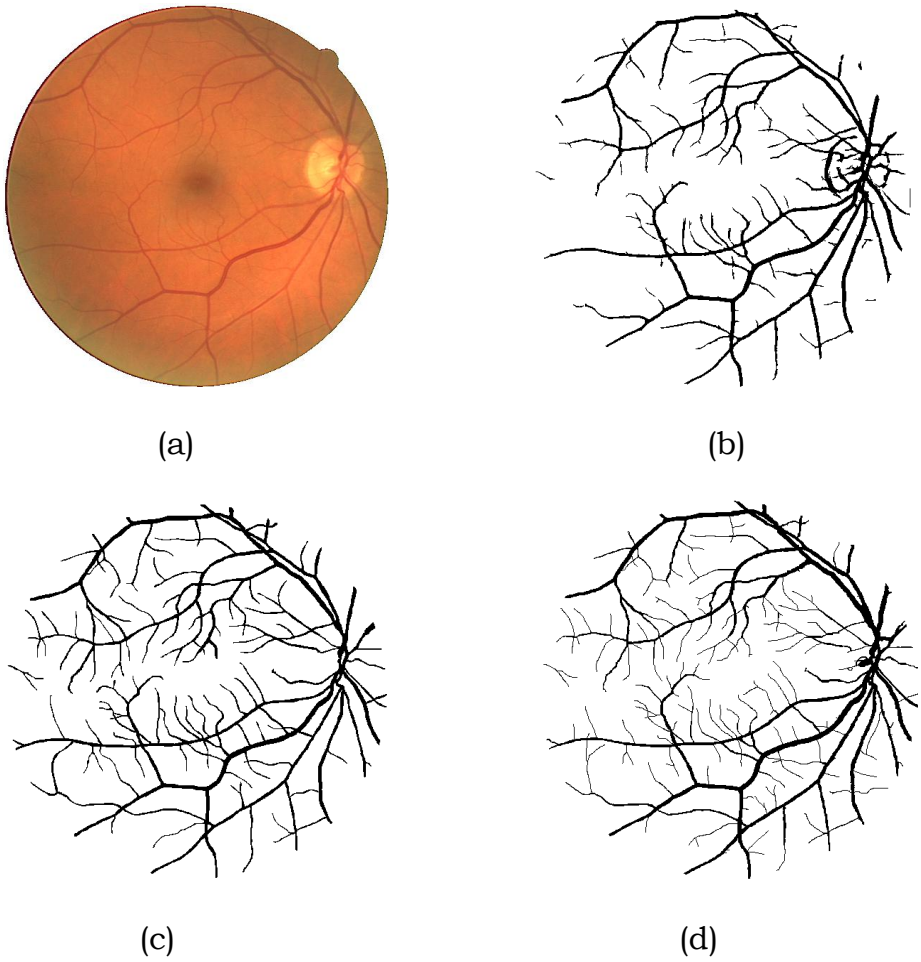

Fig.3.10. Result produced by the proposed HMLRE Method and Manual Segmentations (Sets A and B) for an Image from the DRIVE Database. (a) Normal Retinal Images. (b) Segmentation Result of HMLRE Method. (c) Set A (d) Set B.

first fundus image is 0.9694 and 0.9568 for the second fundus image. The manual segmentations of the two observers are also shown.

In Fig. 3.12 retinal images from STARE database are taken. To evaluate the performance of the HMLRE method, specifically a normal retinal image and a non-uniform illuminated image with obscure blood vessel appearance are considered. The results of HMLRE method are compared with the groundtruth images of the first

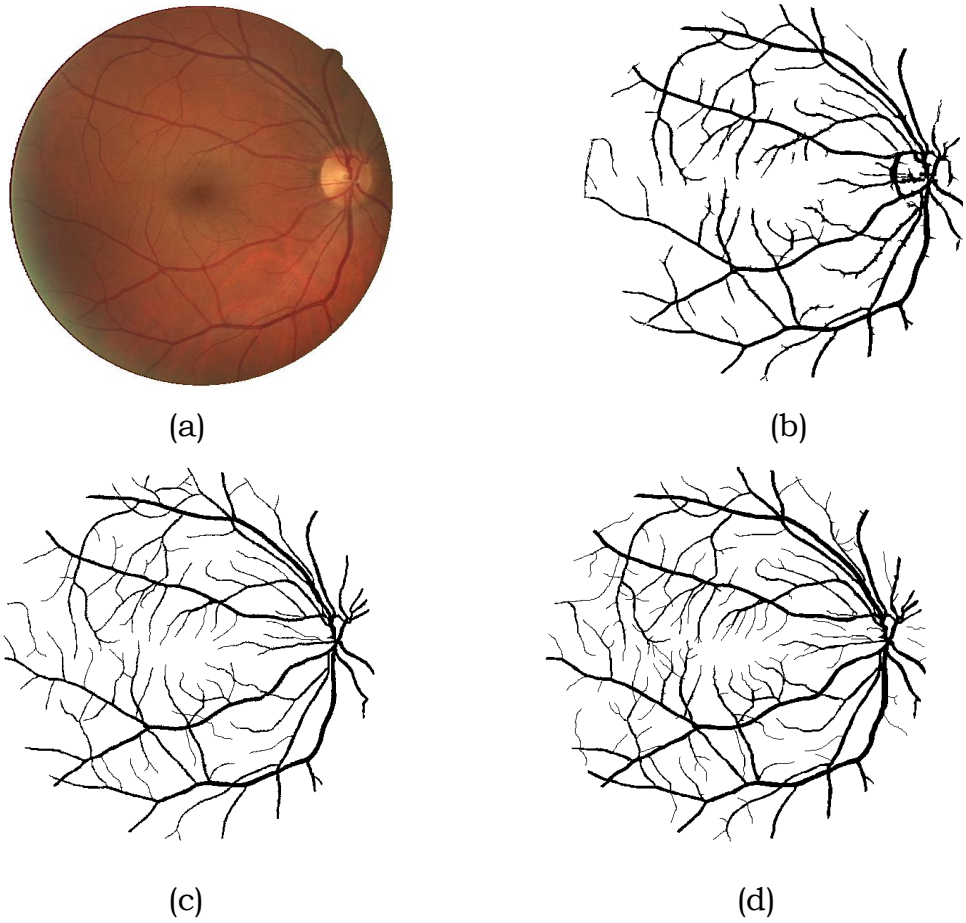

Fig.3.11. Results produced by the proposed HMLRE Method and Manual Segmentations (Sets A and B) for an Image from the DRIVE Database. (a) Normal Retinal Images. (b) Segmentation Results of HMLRE Method. (c) Set A (d) Set B.

observer and with the results of Hoover *et al.* [20] and Chanwimaluang *et al.* [24]. First column results of Fig. 3.12 are originated from a normal retinal image and the second column results are derived from a non-uniform illuminated retinal image with obscure blood vessel appearance. The author has implemented the algorithm

of [24]; whereas the results of [20] are taken from their website[1]. For normal retinal image the algorithms in [20] and [24] attain maximum accuracies of 0.9374 and 0.9221 respectively. However, the result of the HMLRE method shows a significant improvement with maximum accuracy of 0.9586. The accuracy of the proposed HMLRE method for the non-uniform illuminated image with obscure blood vessel appearance shown in the second row is 0.9730. Even though, the brightness of the fundus image reduces radially outwards, the performance of HMLRE method is quite satisfactory not only in the bright central region but also in the dark outermost one. This is owing to the use of both red and green channels of the same fundus image, thus making proposed HMLRE method more robust to non-uniform illumination and contrast. For the same image the maximum accuracies for methods in [20] and [24] are 0.9275 and 0.9513 respectively.

The ROC curves of the proposed HMLRE method, author implementations of the verification based multi threshold probe of Jiang *et al.*[51], matched filter of Chaudhuri *et al.* [18] for both the databases are shown in Figs. 3.13(a) and (b). The manual segmentations from set A of DRIVE database are used as groundtruth. The performance human observer is measured using the manual segmentations from set B and provides only one true/false positive fraction pair that is indicated as a point in the ROC graph (Fig. 3.13(a)). The first observer's manual segmentations are used as

[1]http://www.parl.clemson.edu/stare/probing/

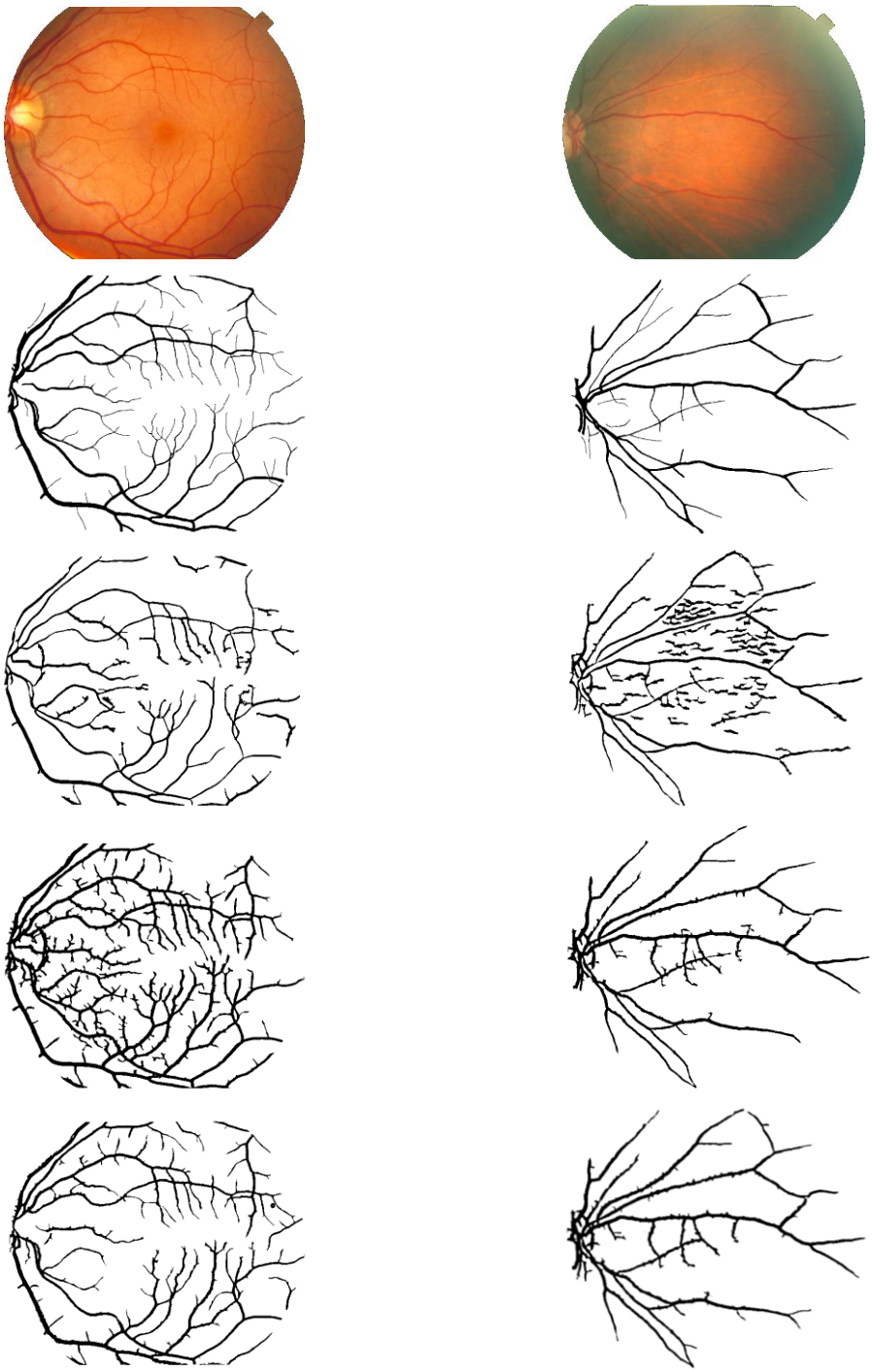

Fig.3.12. Results Produced by the Proposed HMLRE Method for Images from the STARE Database. First Row: Example Images; Second Row: Hand-Labeled Groundtruth ([20]); Third Row: Results of Hoover *et al.* [20]; Fourth Row: Results of Chanwimaluang *et al.* [24]; Fifth Row: Results of HMLRE Method.

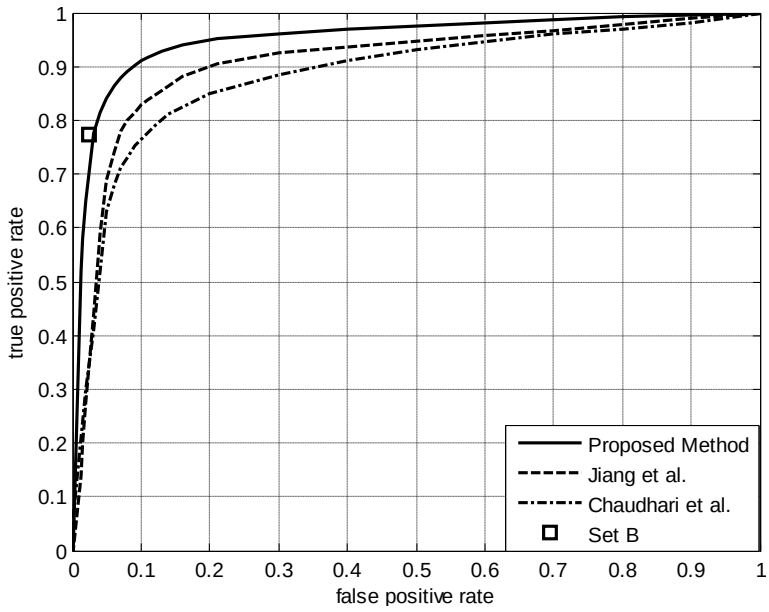

Fig.3.13. (a) ROC Curve for Classification on the DRIVE Database. The point marked as '□' corresponds to set B, the second set of manual segmentations. The HMLRE Method has A_z =0.9518.

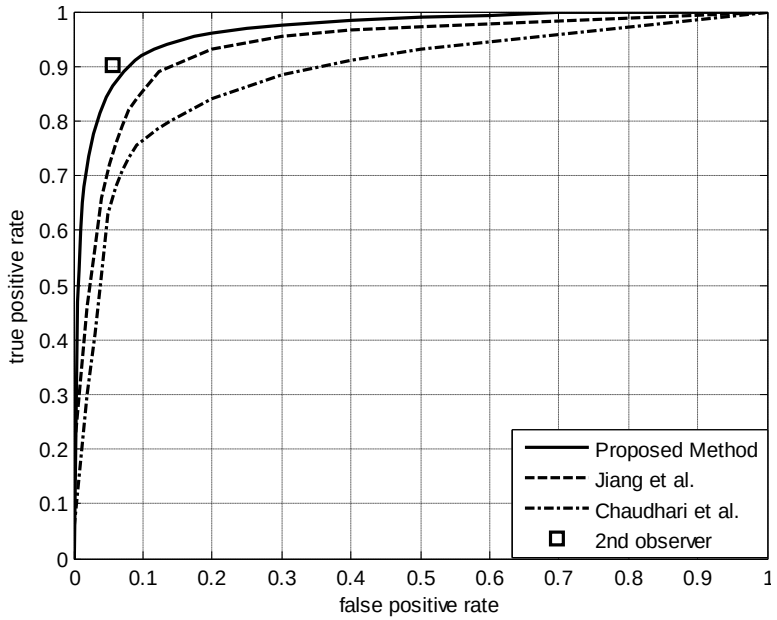

Fig.3.13. (b) ROC curve for classification on the STARE database. The point marked as '□' corresponds to the second observer's manual segmentations. The method has A_z = 0.9602.

Table 3.1 Results for Different Blood Vessel Extraction Methods and a Second Human Observer.

Segmentation Method	**Database**				**Comment**
	DRIVE		**STARE**		
	A_z	**Accuracy**	**A_z**	**Accuracy**	
Staal *et al.*	0.9520	0.9441	0.9614	0.9516	Supervised
Soares *et al.*	0.9614	0.9466	0.9671	0.9480	Supervised
HMLRE method	**0.9518**	**0.9470**	**0.9602**	**0.9549**	**Unsupervised**
Jiang *et al.*	0.9327	0.8911	0.9298	0.8976	Unsupervised
Chaudhuri *et al.*	0.9103	*	0.8987	*	Unsupervised
Lam *et al.*	*	*	0.9392	0.9474	Unsupervised
2nd. observer	*	0.9473	*	0.9349	*

*- Not available

groundtruth for the STARE database, and the true/false positive fraction pair of second observer is shown as a point on the ROC graph (Fig. 3.13(b)).

Table 3.1 compares the proposed approach with the most recent methods in terms of area under ROC and accuracy. The performance of the vessel segmentation method of Staal *et al.* [49] is taken from [48]. The performance of the vessel segmentation method in Lam *et al.* is taken from [97]. The area under ROC (A_z) of the HMLRE method is less when compared to supervised methods [48-49]. The reason is that supervised methods learn from the manual segmentations and they are able to give in accurate results near the edge of groundtruth region. Hence in the ROC curves, the rise in the true positive rate does

not lead to a large rise in the false positive rate and the supervised methods are able to yield a better A_z value. In contrast to the supervised methods, the proposed HMLRE method is more robust in the abnormal regions and can avoid segmenting false vessels in these regions. It is able to yield a solution very closer to the groundtruth. Thus the HMLRE method produces the highest accuracy among others, including supervised methods and gives a ROC curve closest to the true/false positive fraction pair from the second observer.

The proposed HMLRE method is implemented in MATLAB 7.4 on a core 2 Duo 1.8 GHz PC with 1GB memory. The blood vessel segmentation for an image from DRIVE or STARE database requires about 8 seconds, while Staal's method needs 900 seconds on a 1GHz PC and Soare's method requires 180 seconds on a 2GHz PC.

3.4. CONCLUSIONS

In this chapter, a novel approach for the segmentation of blood vessels in digital fundus images is presented. The proposed HMLRE method takes into account the advantages of both red and green channels of a fundus image and the relative local entropy based thresholding. The intensity information of the red channel is utilized for two reasons: 1) To enhance the visual appearance of fundus images in case of non-uniform illumination and 2) To attain better performance of blood vessel segmentation. Combining the advantages of red and green channels i.e. brightness in the red channel and high contrast in the green channel, results in the reduction of the contrast between lesions and the fundus background. Local relative entropy

thresholding algorithm, which takes into account the spatial distribution of gray levels, performs efficiently in distinguishing enhanced vessel segments from the background as it can maintain the structure details of an image. Performance evaluated in terms of area under ROC and accuracy shows that the proposed unsupervised method is better than the existing unsupervised approaches and matches the supervised approaches.

The HMLRE method performs very well in segmenting blood vessels in pathological regions and also extracting thinner vessels even in low contrast regions as the intensity information of both red and green channels is used. However, Fig. 3.10 shows that, there is still room for improvement for detecting the finer vessels. Another difficulty of the proposed method is that in some images border of the optic disk is mis-detected as blood vessel. The future work aims to solve these challenges.

It is essential to obtain large datasets with groundtruth for developing robust solutions to be used for vessel segmentation that can be employed in diabetic screening programmes. However, this is difficult to realize as the groundtruth generation is a tedious process that demands patience. As supervised approaches need part of the available dataset to be employed for training to segmentation, it results in decrease of the actual test set size. These approaches can make it difficult to fully analyse and standardize different methods and obstruct the identification of robust methods for deployment in mass screening programmes. Unsupervised techniques for segmentation, such as the proposed HMLRE method, are hence quite

attractive in this scenario. The HMLRE method exhibits the following features:

- low computational cost
- fast
- high accuracy
- robustness with respect to camera, lighting conditions and the presence of pathologies.